LANGMUIR Article
Cite This: Langmuir 2018, 34, 10187−10196
pubs.acs.org/Langmuir

Insight into the Synergistic Effect on Selective Adsorption for Heavy Metal Ions by a Polypyrrole/TiO_2 Composite

Jie Chen,[†] Mengting Yu,[†] Caiyun Wang,[‡] Jiangtao Feng,*[,†] and Wei Yan*[,†]

[†]Department of Environmental Science and Engineering, State Key Laboratory of Multiphase Flow in Power Engineering, Xi'an Jiaotong University, Xi'an 710049, P. R. China

[‡]ARC Centre of Excellence for Electromaterials Science, Intelligent Polymer Research Institute, AIIM Facility, University of Wollongong, North Wollongong, NSW 2500, Australia

Supporting Information

ABSTRACT: Polymer/metal oxide composites are promising candidates for the treatment of water pollution. Adsorption selectivity as well as a large adsorption capacity are two key factors for treating wastewater containing multiple ions. Herein, a $PPy^+/TiO_2(O^-)$ composite with a heterojunction structure was first discovered to have novel selectivity toward heavy metal ions. An interesting self-doping nature of $TiO_2(O^-)$ together with SO_4^{2-} for PPy^+ was reported. This interesting structure contributed to an impressive selective adsorption capability with an ascending order of Zn^{2+} > Pb^{2+} ≫ Cu^{2+} in a ternary ion system, where the adsorption for Cu^{2+} could be almost suppressed. Through the designed adsorption experiments and characterization techniques including Fourier transform infrared, thermogravimetric analysis, and X-ray photoelectron spectroscopy, a universal synergistic mechanism for $PPy^+/TiO_2(O^-)$ composite was first proposed and confirmed. The doping and dedoping of metal oxide (dopant) from the polymer dictates the adsorption selectivity, where the selectivity is determined by the interaction between TiO_2 and heavy metal ions. This work may provide some useful guidelines for designing adsorbents with selectivity toward specific heavy metal ions.

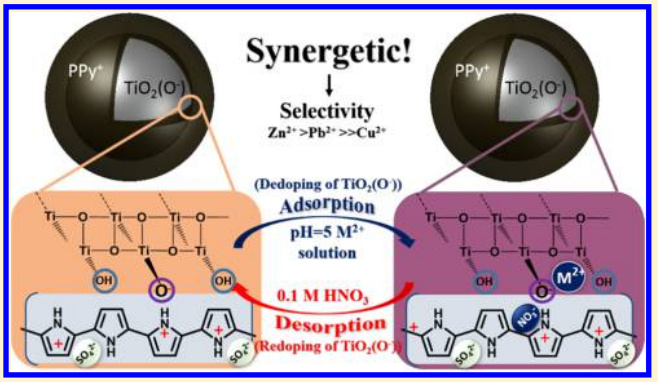

INTRODUCTION

Water pollution with heavy metal ions produced from the industry of mining, painting, car radiator manufacturing, batteries, and metal plating is increasingly becoming a significant environmental problem.[1] Adsorption is regarded as a prospective treatment for heavy metal ions due to its low cost, simplicity, and easy operational conditions and has attracted wide attention from academic and industrial areas.[2−4] However, several kinds of heavy metal ions can coexist in natural and industrial water environments. These ions compete for adsorption sites, leading to a decreased adsorption capacity.[3,5] Therefore, in addition to the large adsorption capacity, the selective adsorption ability of the adsorbent is especially important in the treatment of wastewater.[6]

Another important aspect to consider is the common synergistic phenomenon in the composites, which demonstrated many interesting properties such as solubility and hydrophilicity compared to each component.[7−11] Thus, design and application of polymer/metal oxide composite have attracted attention for wastewater treatment due to the interesting synergistic effect between polymer and metal oxides.[6−11] Hu et al.[12] synthesized graphene oxide/polypyrrole (GO/PPy) composites for highly selective enrichment of U(VI) from aqueous solutions, and the selective adsorption capacity of U(VI) on GO/PPy composites was much higher than those of U(VI) on GO and PPy due to the synergetic adsorption. Khan et al.[13] prepared a fibrous-type polymeric−inorganic composite material: polypyrrole/Th(IV) phosphate applied as a Pb(II) ion selective membrane electrode. Selectivity was investigated in some binary separations like Pb(II)−Zn(II), Pb(II)−Ni(II), Pb(II)−Cu(II), and Pb(II)−Cd(II) on its column. The results suggested that synergetic effect between PPy and Th(IV) phosphate increases the selectivity toward Pb(II). Even though composite synthesis for adsorption purposes is a subject undergoing intense study, the mechanism of the synergistic effects in these studies was only inferred without detailed investigation. Understanding the mechanism behind the synergistic effects is very important, which can provide a guideline to design an adsorbent with improved adsorption capacity.

In this work, we selected PPy and TiO_2 as the subjects for studying the synergistic effects. Specifically, conjugated polymer polypyrrole (PPy) is a promising candidate due to its novel conjugated structure and redox properties, offering a

Received: June 13, 2018
Revised: July 28, 2018
Published: August 3, 2018

DOI: 10.1021/acs.langmuir.8b01987
Langmuir 2018, 34, 10187−10196

rich electrochemical chain that undergoes ion doping and dedoping on the pyrrolylium nitrogen (Scheme S1), which may additionally experience interaction and synergistic effect with metal oxides.[14−18] Metal oxides have demonstrated a selective adsorption affinity to some heavy metal ions such as Mn oxides to Cu(II), Fe oxides to Pb(II), whereas Zn(II) can be specifically attracted by Si oxides.[19] The synergistic effect between PPy and metal oxides may be expected to produce a material with selective ion uptake. Even though there have been some reports about PPy/metal oxides for heavy metal adsorption,[20−23] the adsorption capacity in multiple metal ions solutions is limited.

Herein, this work aims to gain insight into the synergistic mechanism between polymer and metal oxide for the selective adsorption of metal ions. The redox states, structure, textural properties, and interaction between PPy and TiO_2 were characterized. Various adsorption experiments, including kinetic, single, and multicomponent isotherms, were designed and conducted to reveal the individual and competitive adsorption properties for Pb(II), Zn(II), and Cu(II). Finally, the mechanism of the synergistic effect between PPy and TiO_2 was first proposed based on the pH experiments as well as characterization results from Fourier transform infrared (FT-IR), thermogravimetric analysis (TGA), and X-ray photoelectron spectroscopy (XPS). This work provides a general understanding of the mechanism for the synergetic effect between a polymer and metal oxide for the selective adsorption of heavy metal ions. The proposed mechanism may be of great value in guiding the design of adsorbents with selectivity toward certain heavy metal ions and are widely used in the removal of pollutants from wastewater.

EXPERIMENTAL SECTION

Materials. Chemicals used in this study were of analytical grade and purchased from Sinopharm Chemical Reagent Co., Ltd. Pyrrole was distilled twice and stored in the dark before use. The standard heavy metal solutions were prepared from $Pb(NO_3)_2$, $Cu(NO_3)_2{\cdot}3H_2O$, and $Zn(NO_3)_2{\cdot}6H_2O$ with deionized water.

Synthesis of PPy, TiO_2, and PPy/TiO_2 Composite. The PPy/TiO_2 composite doped with H_2SO_4 was synthesized using in situ chemical oxidative polymerization.[24] The TiO_2 was prepared through sol−gel method. *N*-Propanol and tetrabutyl titanate (AR) at a volume ratio of 5:2 were carefully charged into H_2SO_4 solution (200 mL, 0.24 mol/L) and stirred for 24 h. The formed TiO_2 suspension solution was cooled down to 5 °C in the dark before 0.675 mL of pyrrole monomer was added. Then, $FeCl_3$ solution (25 mL, 1.0 mol/L) was dosed dropwise into the mixture and stirred for another 24 h in dark. The formed dark composite was filtrated and washed with 0.01 mol/L H_2SO_4 solution several times to remove the oligomer and other impurities. For comparison, pure TiO_2 was prepared using the same procedure but without adding pyrrole monomer and $FeCl_3$; pure PPy was synthesized using the same procedure but without adding TiO_2.

Characterization. Fourier transform infrared (FT-IR) spectra of PPy, TiO_2, and PPy/TiO_2 composite were performed on a BRUKER TENSOR 37 FT-IR spectrometer by the KBr pellet method over a range of 4000−400 cm^{-1}. X-ray photoelectron spectroscopy (XPS) spectra were recorded on a Kratos Axis Ultra DLD with an Al monochromatic X-ray source (1486.71 eV). All binding energies were referenced to the C 1s hydrocarbon peak at 284.6 eV. The ζ-potential investigations were conducted on a Malvern Zetasizer Nano ZS90. Thermogravimetric analysis (TGA) was investigated on a Setaram Labsys Evo in N_2 flow, and the heating rate was 10 °C/min. X-ray diffraction (XRD) patterns were acquired on an X'Pert PRO Diffractometer with a wavelength of 1.5406 Å (Cu Kα radiation method) over a range of 10−80°. The N_2 adsorption and desorption isotherms were recorded on a Builder SSA-4200 at 77 K and the specific surface area, total pore volume, and average pore radius were calculated using a Builder analysis software. Scanning electron microscopy (SEM) and energy-dispersive X-ray spectrum (EDS) was performed on a JSM-6700F. Transmission electron microscopy images (TEM) were recorded on a JEM model 2100 electron microscope. The concentrations of heavy metal ions were determined using an inductive coupled plasma emission spectrometer (ICPE-9000, Shimadzu).

Adsorption Experiments. In all adsorption experiments, the dose of adsorbent was 2 g/L and the volume of heavy metal solution was 20 mL. All experiments were conducted in a shaker at a constant temperature, and the agitation speed was kept at 200 rpm. To avoid the influence of precipitation of metal ions on the adsorption, the solution pH was kept at 5.

In the kinetic experiment, the composite was dosed in 400 mg/L Pb^{2+}, Zn^{2+}, and Cu^{2+} solutions, respectively, with various contact times (0−180 min). In the single-ion isotherm investigations, the composite was dosed in Pb^{2+}, Zn^{2+}, and Cu^{2+} solutions of various initial concentrations for 3 h at 15, 25, and 45 °C, respectively. For Pb^{2+} adsorption, the initial concentration was 100, 200, 300, 400, 600, and 800 mg/L, whereas for Zn^{2+} and Cu^{2+} adsorption, the initial concentration was 10, 50, 100, 200, 400, and 600 mg/L. In the multiple-ion isotherm investigations, the composite was dosed in a mixed solution of Pb^{2+}, Zn^{2+}, and Cu^{2+} with an initial concentration of 50, 100, 200, 300, and 400 mg/L at 25 °C for 3 h. The pH experiment was conducted in the solutions with the initial pH from 1 to 5 and an initial heavy metal ion concentration of 200 mg/L for 3 h. The pH used was adjusted using HNO_3 or NaOH concentrated solution. (**Caution!** The HNO_3 and NaOH solutions are highly corrosive!)

The adsorption capacity and recycle efficiency was calculated as follows

$$Q_e = \frac{(C_0 - C_e)V}{m} \tag{1}$$

$$\text{recycle efficiency} = \frac{Q_{e,n}}{Q_{e,0}} \times 100\% \tag{2}$$

where Q_e (mg/g) is the equilibrium adsorption capacity, C_0 and C_e (mg/L) are the initial and equilibrium concentrations of heavy metal ions, respectively, m (g) is the weight of adsorbent, V (L) is the solution volume, $Q_{e,n}$ represents the adsorption capacity at the nth cycle, whereas $Q_{e,0}$ represents the adsorption capacity before the recycle.

RESULTS AND DISCUSSION

Characterization. The structure of PPy/TiO_2 composite was illuminated by the FT-IR spectra as shown in Figure S1, and the main characteristic bands are listed in Table S1. For comparison, the spectra of TiO_2 and PPy were also presented. TiO_2 showed only two broad peaks at 3419 and 400−700 cm^{-1}. After being coated with PPy, it clearly exhibited the combination of typical characteristic peaks of PPy (1551, 1457, 1317, and 1056 cm^{-1}) and TiO_2 (400−700 cm^{-1}), evidencing the successful formation of PPy/TiO_2 composite. In addition, the presence of a strong peak situated at 1056 cm^{-1} was ascribed to C_β−H, suggesting an $\alpha-\alpha$ linking and regular polymerization of PPy.[18] The second dopant ion SO_4^{2-} was also detected. However, it was also noticed that the peaks assigned to hydroxyl at 3419 and 1629 cm^{-1} of TiO_2 and those for Py ring (1524, 1442, 1284 and 1025 cm^{-1}), respectively, shifted to lower or higher wavenumbers, confirming the conclusion from the density functional theory (DFT) calculations[25] that PPy is a p-type semiconducting polymer, which donates its electron cloud density to TiO_2, making TiO_2 to be an n-type material in the PPy/TiO_2 composite. Therefore, following the DFT and the FT-IR results from

DOI: 10.1021/acs.langmuir.8b01987
Langmuir 2018, 34, 10187−10196

Scheme 1. Synergistic Adsorption between PPy and TiO_2 in the PPy/TiO_2 Composite for the Selective Adsorption for Heavy Metal Ions

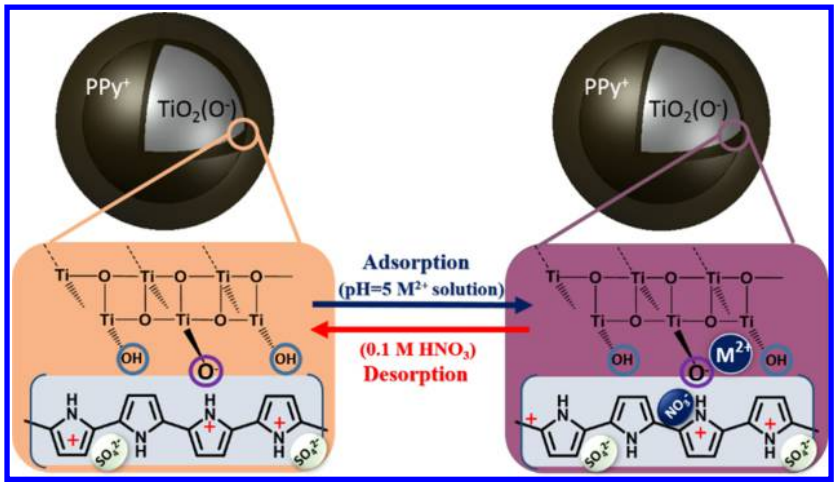

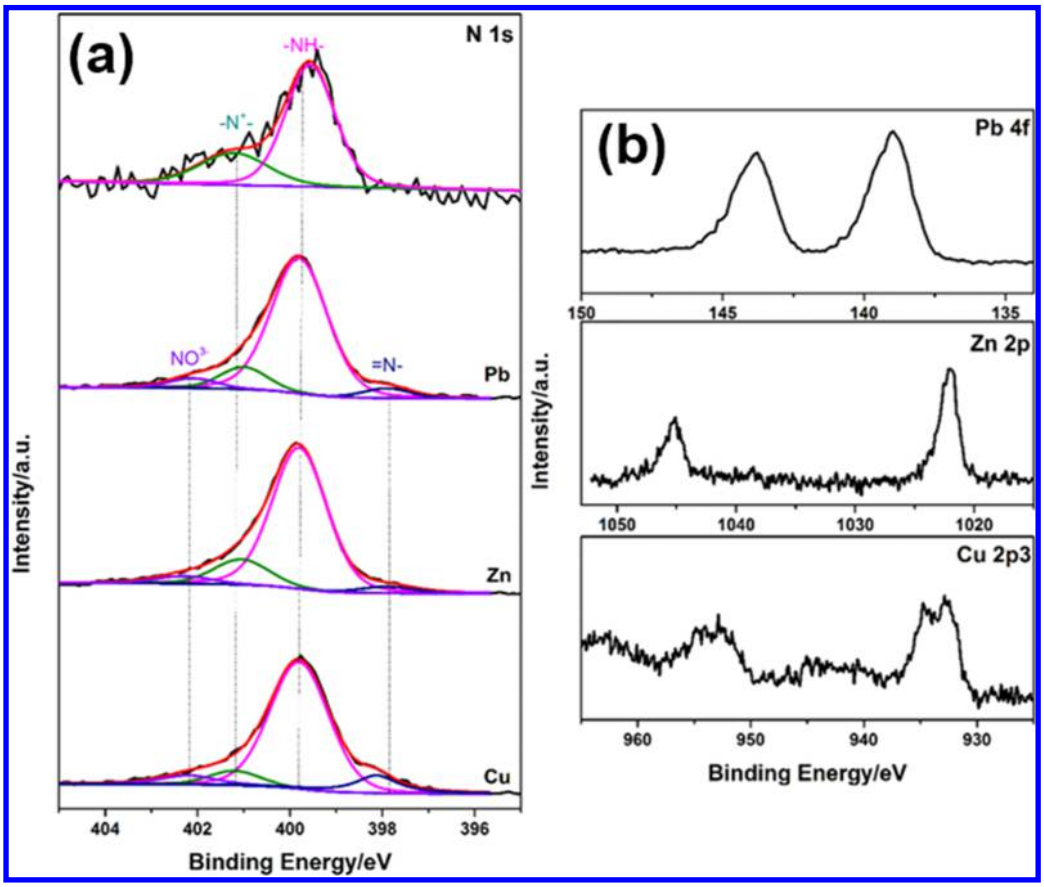

Figure 1. (a) XPS N 1s core level spectra of PPy/TiO_2 composite before and after the adsorption of Pb^{2+}, Zn^{2+}, and Cu^{2+}. (b) Pb 4f, Zn 2p, and Cu $2p^3$ core level spectra of PPy/TiO_2 composite after the adsorption of Pb^{2+}, Zn^{2+}, and Cu^{2+}.

the PPy/TiO_2 composite, we proposed for the first time that TiO_2 could be a dopant, acting through the hydroxyl to dope and undergo charge-transfer (CT) interactions with PPy in the PPy/TiO_2 system. The CT interaction model between PPy and TiO_2 proposed herein (Scheme 1) may well explain the mechanism of the synergistic adsorption between PPy and TiO_2 and the selective adsorption for heavy metal ions discussed in the later sections.

The N 1s XPS spectra shown in Figure 1 also confirm the p-type doping state of PPy ($PPy^+(X^-)$). It can be deconvoluted into two peaks, which reveals the presence of a secondary component at 401.3 eV for the positively charged nitrogen ($-N^+-$) and a major component at 399.9 eV for the pyrrolylium nitrogen ($-NH-$).[18] It also verified that PPy was completely in its oxidation state. In addition, the proportion of positively charged nitrogen in the composite is calculated to be 31.2% according to the peak area, suggesting a doping level of 31.2% for PPy.[18] This doping feature is also confirmed by the ζ-potential investigation (Figure 2). The pH of zero point charge (pH_{pzpc}) of the composite was 10.3, close

DOI: 10.1021/acs.langmuir.8b01987
Langmuir 2018, 34, 10187−10196

to that of 10.4 for PPy, indicating the positively charged nature of the pyrrolylium nitrogen.[15]

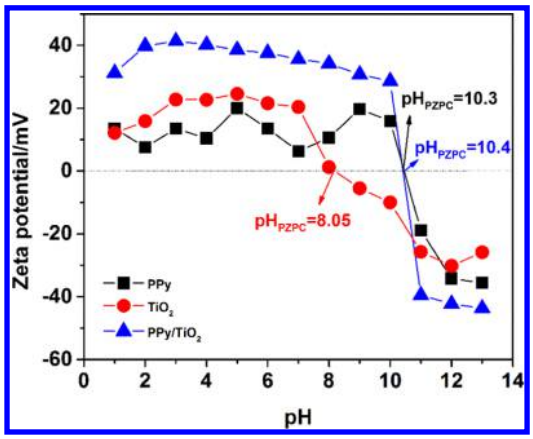

Figure 2. ζ-Potentials of PPy, TiO_2, and PPy/TiO_2 composite in different pH and the pH of zero-point charge.

The CT interaction was effected by thermal degradation, and $PPy^+(X^-)$ began to deprotonate and dedope to deprotonated-PPy when it was heated to a certain temperature.[26] Therefore, to further confirm the CT interaction in the composite between TiO_2, PPy, and dopant ions ($TiO_2(O^-)$ and SO_4^{2-}), thermogravimetric analysis (TGA) was carried out and shown in Figure S2. PPy/TiO_2 displayed a three-stage degradation process: the first weight loss from room temperature to 300 °C is assigned to the loss of hydroxyls and the adsorbed water;[27] the second weight loss interval between 300 and 600 °C is ascribed to the loss of the doped ions SO_4^{2-}, which agrees with the results for $PPy^+(Cl^-)$ that the loss of chloride species started from slightly higher than 300 °C;[26] the final weight loss above 600 °C may be due to the further thermal decomposition of PPy. This weight loss process is also verified by the proportion losses of each component in the samples from the TGA result (Table 1). The content of SO_4^{2-} in the PPy was calculated to be about 18.73 w/w% based on a doping level of 31.2% from the XPS result (for calculation details, please see the Supporting Information), which fits well with the second weight loss interval of around 19.02 w/w% in the TGA experiment. In addition, the SEM–EDS were performed for the elemental analysis to confirm the existence of SO_4^{2-} (Figure S3 and Table S2), and its content (2.58 w/w%) fits well with the TGA results (the content of SO_4^{2-} and OH^- in TGA was calculated to around 7.5 w/w%). From the TGA study, the content of TiO_2 in the composite was more than 70%, suggesting that TiO_2 may play a more important role in the adsorption.

To better characterize the structure of PPy/TiO_2 composite, the XRD spectra of PPy and TiO_2 were also investigated and are shown in Figure S4. Amorphous PPy and anatase TiO_2 with characteristic peaks at 25.3, 37.8, and 48.1° can be confirmed.[28] After being covered with PPy, those three characteristic peaks almost disappeared, suggesting that the anatase TiO_2 was completely covered with amorphous PPy.[29] This core–shell like feature is also supported by the N_2 adsorption–desorption results (Figure 3). The textural

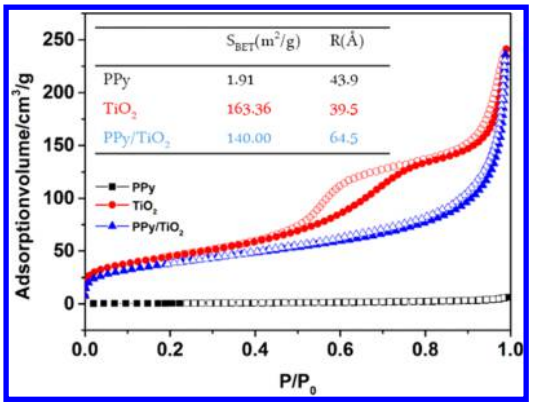

Figure 3. N_2 adsorption and desorption isotherms of PPy, TiO_2, and PPy/TiO_2 composite.

parameters are listed in Table S3. The surface area and pore volume of TiO_2 were extensively reduced after the modification with PPy, which results from the blocking with PPy. The core–shell like structure was confirmed by the SEM and TEM images as shown in Figure S5. The lattice fringe of TiO_2 can be clearly observed in the core of the composite, which was covered by an amorphous shell of PPy. This structure was very stable, and TiO_2 was still tightly covered by PPy after dedoping (Figure S5c). No isolated TiO_2 was observed. The pore diameter of the composite was around 6.45 nm, much larger than the radius of heavy metal ions (0.97 Å for Pb^{2+}, 0.74 Å for Zn^{2+}, and 0.7 Å for Cu^{2+}), indicating that the ions can diffuse through PPy to reach TiO_2 without resistance. It is also interesting to find that the isotherm of TiO_2 was changed from type II to type I after PPy modification, further confirming the structural changes of the pores.[30] Nevertheless, this composite still showed a surface area of 140.0 m^2/g, providing sufficient sites for heavy metal adsorption.

Adsorption Investigation. The detailed adsorption properties including kinetic, regeneration investigation, and field sample analysis were carried out and shown in Section S5 in the Supporting Information. The results showed that PPy/TiO_2 composite is a promising adsorbent for adsorption. The

Table 1. Proportion of Each Component in PPy, TiO_2, and PPy/TiO_2 Composite before and after Adsorption

	temperature		
	<300 °C (water/hydroxyl)	300–600 °C (hydroxyl/doping ions)	>600 °C (PPy)
PPy	15.39 w/w% (water)	19.02 w/w% (doping ions)	5.80 w/w% (PPy)
TiO_2	14.57 w/w% (water/hydroxyl)		
PPy/TiO_2	12.15 w/w% (water/hydroxyl)	7.50 w/w% (hydroxyl/doping ions)	4.84 w/w% (PPy)
PPy/TiO_2 Pb	14.17 w/w% (water/hydroxyl)	11.38 w/w% (hydroxyl/doping ions)	9.06 w/w% (PPy/M^{2+})
PPy/TiO_2 Zn	16.04 w/w% (water/hydroxyl)	9.51 w/w% (hydroxyl/doping ions)	8.23 w/w% (PPy/M^{2+})
PPy/TiO_2 Cu	16.04 w/w% (water/hydroxyl)	9.51 w/w% (hydroxyl/doping ions)	4.37 w/w% (PPy/M^{2+})

DOI: 10.1021/acs.langmuir.8b01987
Langmuir 2018, 34, 10187–10196

adsorption equilibrium can be achieved within 5 min for Zn^{2+}, 7 min for Cu^{2+}, and 40 min for Pb^{2+}, evidencing a fast adsorption. It can be recycled using HNO_3 and NaOH, which has low cost and easy to operate. Thus, it can be effectively used in field conditions.

To understand the adsorption properties and selective adsorption nature, and quantify the maximum adsorption capacity of PPy/TiO_2 composite, isotherm studies at different temperatures in single- and multicomponent (ternary) systems were carried out (Figure S6).[31] The equilibrium experimental data were fitted using typical Langmuir[32] and Freundlich[33] models to illuminate the adsorption affinity and capacity, whereas Dubinin−Radushkevich[34] and Temkin[35] models were used to estimate the adsorption free energy and heat.[36] Relevant parameters and details about the models are summarized in Tables 2 and S4. Considering the value of R^2 and the accuracy of the Q_m calculated, the equilibrium data can be well described by the Langmuir model, followed by the Freundlich and Temkin models in all the cases, whereas the Dubinin−Radushkevich model is the least capable of predicting the adsorption. Therefore, the following discussions were mainly based on the Langmuir fitting results.

From the Langmuir model, PPy/TiO_2 composite showed an outstanding maximum adsorption capacity up to 0.677 mmol/g for Pb^{2+}, 1.197 mmol/g for Zn^{2+}, and 0.141 mmol/g for Cu^{2+}, respectively, in single-ion solutions. The absorption capacities of this material were competitive with the recently reported adsorbents (Table S5, Supporting Information). Moreover, it is noticeable that Q_m in the Pb^{2+} and Zn^{2+} adsorption spectra increased steadily with temperature, which may result from the ionic exchange adsorption nature.[22] This phenomenon was also reported for other PPy-based adsorbents such as a PPy/chitin composite that adsorbed Pb^{2+} and Cd^{2+} [37] and PPy/sawdust composite used for Zn^{2+} adsorption.[38] In contrast, the temperature did not obviously influence the Cu^{2+} adsorption. The adsorption of Cu^{2+} may have a different adsorption mechanism with Pb^{2+} and Zn^{2+}.

The multiple-ion solution was applied to further investigate the selective adsorption property of PPy/TiO_2 composite, which is important in adsorption engineering but is rarely reported.[6] The adsorption isotherm data could be well described by Langmuir model, indicating that the adsorption in the multi-component system was still monolayered.[39,40] It is reasonable that the adsorption capacities (Q_m) deteriorated due to the competition between heavy metals for the adsorption sites. To better correlate the data obtained from single-metal equilibrium with the multimetal data, the P factor, a dimensionless parameter shown in eq 3, is introduced.

$$P = \frac{Q_{max,single}}{Q_{max,multiple}} \quad (3)$$

where $Q_{max,single}$ and $Q_{max,multiple}$ are the maximum adsorption capacity of heavy metals in single- and multicomponent systems. Obviously, the higher the affinity toward one metal, the higher the value of P is; and the higher selectivity the composite has, the bigger is the difference in the P values for different metal ions. The P values of the composite for three heavy metals are presented in Table 2. It is interesting to see that the P values showed a descending order of $Zn^{2+} > Pb^{2+} \gg Cu^{2+}$, and the adsorption of Cu^{2+} was almost completely forbidden in the multicomponent system, suggesting that PPy/TiO_2 composite can be applied to separate and recycle heavy metals from Cu^{2+}-rich electroplating effluent without the influence and competition of Cu^{2+}. It should be noted that there is not a mechanism about selective adsorption that can perfectly explain all the experimental results yet, and the reported results contradicted each other in the previously reported work. For example, Xu et al.[41] reported the selective adsorption of heavy metals was in the order of Cu(II) > Co(II) > Ni(II) for a SG−H_2L^2 composite, and they suggested that it may be caused by the cationic radius, hydration energy, and acidity/basicity of the interactive species in the adsorption process. However, contradicting results were observed by Ali et al.[42] that the selective adsorption order for a Mn−MoS_4 composite followed the order $Hg^{2+} > Ag^{+} > Pb^{2+} > Cu^{2+} > Cd^{2+} > Ni^{2+} > Zn^{2+} > Co^{2+}$, in which the selectivity is based on the Hard−Soft−Acid−Base theory. In addition, Ag^{+}, which carries only one positive charge, outperforms other ions with greater charges, challenging the theory that more charged ions would have higher adsorption priority. Another contradicted result was obtained by Chandra et al.[43] A selective adsorption capability of $Hg^{2+} > Cu^{2+} > Cd^{2+} > Pb^{2+} > Zn^{2+}$ was observed in PPy. However, a totally different selectivity of $Hg^{2+} > Zn^{2+} > Cd^{2+} > Pb^{2+} > Cu^{2+}$ was achieved for polypyrrole/reduced graphene oxide composite. Herein, a different phenomenon was reported for a PPy/TiO_2 composite, which had selective adsorption capability in the order of $Zn^{2+} > Pb^{2+} \gg Cu^{2+}$, even though Zn^{2+} has a smaller ionic radii and Pauling electronegativity (0.74 and 1.65 nm) than Pb^{2+} (0.97 and 2.33 nm) and Cu^{2+} (0.7 and 1.9 nm), suggesting that the selectivity of the adsorbent depends on the adsorbent as well as the adsorbate, and the mechanism previously proposed cannot well explain all these situations.

To elucidate the selectivity of PPy/TiO_2 composite, competitive adsorption studies of PPy and TiO_2 was also conducted, all the results are summarized in Figure S6d−i and Table 2. It is interesting to notice that that TiO_2 showed a similar adsorption behavior in a multicomponent system to the PPy/TiO_2 composite. Such a behavior was not observed for PPy. In addition, TiO_2 did show similar selectivity order to that of PPy/TiO_2, which follows $Zn^{2+} > Pb^{2+} > Cu^{2+}$. Therefore, it can be deduced that the selectivity for heavy metals for this composite was determined by TiO_2 instead of PPy. It can be hypothesized that Pb^{2+} and Zn^{2+} are favored by TiO_2 and PPy/TiO_2 composite but not Cu^{2+}, even though PPy has a good affinity toward Cu^{2+}, which can be only adsorbed by PPy by the limited imine groups. However, the reason why a metal oxide has strong affinity toward specific heavy metal ions could not be given. Inspired by the work conducted by Oyetade et al.,[44] which used DFT calculations to simulate the combination of ions with acid-functionalized multiwalled carbon nanotubes on a lattice structure scale, we hypothesize herein that the selectivity of metal oxide to heavy metal ions should be related to the compatibility of the lattice structures of metal oxides with heavy metal ion hydroxide. Further investigation will be the subject of our future work.

From the fitting results of Dubinin−Radushkevich and Temkin model, it can be seen in Figures S7, S8 and Table S4 that the adsorption free energy (E) and heat (B) also followed the increasing trend in temperature, which is consistent with the results from the Langmuir model. However, these two models cannot describe the data well; therefore, the values of the adsorption free energy (E) and heat (B) are not used to determine the adsorption mechanism.

DOI: 10.1021/acs.langmuir.8b01987
Langmuir 2018, 34, 10187−10196

Table 2. Single- and Multicomponent Adsorption Isotherms Parameters Describing the Adsorption of Heavy Metals (Pb^{2+}, Zn^{2+}, and Cu^{2+}) onto PPy/TiO_2 Composite Based on the Langmuir and Freundlich Models[a,b]

			samples													
			PPy/TiO_2									PPy			TiO_2		
			Pb			Zn			Cu			Pb	Zn	Cu	Pb	Zn	Cu
			15 °C	25 °C	45 °C	15 °C	25 °C	45 °C	15 °C	25 °C	45 °C	25 °C	25 °C	25 °C	25 °C	25 °C	25 °C
Langmuir	single	$Q_{m,mass}$	125.79	140.27	237.03	72.65	77.81	83.88	10.32	9.01	9.27	65.27	67.51	40.50	68.13	46.83	15.63
		$Q_{m,mol}$	0.607	0.677	1.145	1.117	1.197	1.29	0.160	0.141	0.145	0.315	1.039	0.633	0.329	0.720	0.244
		K_L	0.0061	0.0046	0.0022	0.0058	0.0068	0.0078	0.0044	0.0073	0.013	0.0017	0.0045	0.0019	0.020	0.0029	0.0010
		R^2	0.996	0.997	0.991	0.996	0.995	0.994	0.997	0.995	0.991	0.991	0.995	0.998	0.980	0.994	0.997
	multiple	$Q_{m,mass}$		65.52			40.38			0		122.06	125.18	124.79	45.38	45.12	0
		$Q_{m,mol}$		0.312			0.621			0		0.0583	1.926	1.950	0.219	0.694	0
		K_L		0.01746			0.00046					0.014	0.019	0.015	0.0039	0.0022	
		R^2		0.994			0.988					0.978	0.993	0.991	0.998	0.999	
		P		**0.467**			**0.519**			**0**		**0.184**	**1.854**	**3.081**	**0.666**	**0.963**	**0**
Freundlich	single	K_F	6.91	5.00	2.23	2.28	2.85	3.52	0.27	0.47	0.98	0.98	2.10	0.504	16.66	0.58	0.10
		$1/n$	0.42	0.48	0.65	0.52	0.50	0.49	0.52	0.44	0.34	0.65	0.57	0.71	0.21	0.62	0.80
		R^2	0.998	0.998	0.963	0.989	0.982	0.986	0.988	0.981	0.922	0.968	0.966	0.989	0.744	0.971	0.790
	multiple	K_F		6.45			0.148					12.37	17.23	13.63	1.15	0.30	
		$1/n$		0.39			0.94					0.38	0.32	0.35	0.64	0.72	
		R^2		0.941			0.979					0.994	0.891	0.917	0.995	0.997	

[a]Langmuir model: $Q_e = \frac{Q_m K_L C_e}{1 + K_L C_e}$, $P = \frac{Q_{max,single}}{Q_{max,mutiple}}$ where Q_e (mg/g) is the adsorption capacity; $Q_{m,mass}$ (mg/g)/$Q_{m,mol}$ (mmol/g) represents the maximum adsorption capacity; K_L (L/mg) is an Langmuir constant related to the affinity between adsorbents and adsorbate; P factor is a dimensionless parameter to estimate the selectivity of heavy metals. [b]Freundlich model: $Q_e = K_F C_e^{1/n}$ where K_F(mg^{1-n} L^n/g) is a constant related to the adsorption capacity of adsorbent when the equilibrium metal ions concentration equals to 1; n states the degree of dependence of the adsorption on the equilibrium concentration.

DOI: 10.1021/acs.langmuir.8b01987
Langmuir 2018, 34, 10187−10196

Synergistic Adsorption and Selective Adsorption Mechanism. Inspired by the interesting selective adsorption properties of PPy/TiO_2 composite, we continued to design and carry out experiments to investigate the mechanism of the synergistic adsorption between PPy and TiO_2, and the selective adsorption mechanism for heavy metals.

Adsorption Sites. FT-IR analyses before and after heavy metal adsorption for TiO_2, PPy, and PPy/TiO_2 composite were performed (Figure S1b–d) to determine the adsorption sites, and the main characteristic peaks are listed in Table S1. For TiO_2, the peaks assigned to hydroxyls at 3419 and 1629 cm^{-1} showed an obvious redshift to higher wavenumbers after adsorbing Pb^{2+}, Zn^{2+}, and Cu^{2+}, suggesting an interaction between the hydroxyls on the surface of TiO_2 and heavy metals.[45] The peak shift of Cu^{2+} was relatively smaller, confirming the result obtained by the competitive isotherm investigation that adsorption of Cu^{2+} was not favorable for TiO_2. As for PPy and PPy/TiO_2 composite, a redshift was clearly observed for the peak ascribed to C–N at around 1442 cm^{-1} as well, and its intensity became very weak after adsorption, indicating a new environment around the pyrrolic nitrogen on the PPy chain.[26] This result may be one of the important evidences for the ionic exchange and dedoping of $TiO_2(O^-)$ during adsorption.

Synergistic Adsorption and Selective Adsorption Mechanism. It is difficult to interpret the selective adsorption order of $Zn^{2+} > Pb^{2+} \gg Cu^{2+}$ for PPy/TiO_2 composite if using the Hard–Soft–Acid–Base theory or the properties of heavy metals only. Therefore, the synergistic adsorption between TiO_2 and PPy in the selective adsorption process was also considered. As we discussed above, $TiO_2(O^-)$ along with SO_4^{2-} acted as dopants and were involved in the charge-transfer interaction with PPy in the composite. However, the unstable oxidization doped state of PPy is relatively easy to dedope or exchange dopants with rich ions such as NO_3^- in the heavy metal ion solution at pH > 3,[46] and some imine could be formed. To illuminate this process, XPS investigations on the composite after adsorption was conducted. The N 1s spectra of PPy/TiO_2 after adsorption are depicted in Figure 1, and the assignments and their ratio of peak area are presented in Table 3 to illustrate the changes of N. It shows an interesting result: a decreased ratio of $-N^+-$, an increased ratio of =N–, and an unchanged ratio of –NH–; confirming a certain degree of dedoping for the composite. However, the TGA results shown in Table 1 inferred that the mass of doping ions (300–600 °C) still increased after adsorption, suggesting that the dedoped ions should be $TiO_2(O^-)$ instead of SO_4^{2-}; some $TiO_2(O^-)$ may be also exchanged by NO_3^-.[26] It is reasonable because SO_4^{2-} has a large size and is relatively hard to dedope from the PPy chain. From the XPS result, another interesting result can be also noticed is that for favorable ions of Pb^{2+} and $Zn^{2+}$by PPy/TiO_2, the dedoping rate was much lower (larger $A(-N^+-)/A(=N-)$) than for Cu^{2+}. It can be inferred that Cu^{2+} may be adsorbed on PPy in a different manner than Pb^{2+} and Zn^{2+}. This is due to the chemical equilibrium between metal ion and PPy, where the dedoping process can be promoted by heavy metal ions if they have the following interaction with PPy

$$PPy(-N^+-)X^- == PPy(=N-) + HX \quad (4)$$

$$PPy(=N-) + Cu^{2+} == PPy(=N-) \rightarrow Cu^{2+} \quad (5)$$

Table 3. Assignment and Ratio of Peak Areas in the XPS N 1s Core Level Spectra of the PPy/TiO_2 Composite after Pb^{2+}, Zn^{2+}, and Cu^{2+} Adsorption[a]

	Pb			Zn			Cu		
assignment[18]	binding energy/eV	ratio of peak area/%	$A(-N^+-)/A(=N-)$	binding energy/eV	ratio of peak area/%	$A(-N^+-)/A(=N-)$	binding energy/eV	ratio of peak area/%	$A(-N^+-)/A(=N-)$
=N–	397.87	4.869	2.264	397.97	4.176	3.971	398.17	5.856	0.771
–NH–	399.77	11.001		399.77	14.104		399.77	7.668	
$-N^+-$	400.97	79.269		401.07	78.168		401.27	76.534	
NO_3^-	402.07	4.861		402.27	3.552		402.17	9.942	

[a]The FWHM is set as 1.4 eV, and the % Lorentzian–Gaussian is set as 20%.

DOI: 10.1021/acs.langmuir.8b01987
Langmuir 2018, 34, 10187–10196

This reaction can be also confirmed by the XPS spectra of Cu 2p, in which the Cu−N can be obviously detected after adsorption (Figure 1b), suggesting the main adsorption site for Cu^{2+} is on the PPy through the imine. The similar shape line was also found in Cu/N-doped TiO_2.[47,47] As for Pb^{2+} and Zn^{2+}, the peaks for Pb−N and Zn−N were overlapped and only hydrated (Pb−O and Zn−O) and nitrated forms can be detected,[48,49] confirming that Zn^{2+} and Pb^{2+} were mainly adsorbed on TiO_2, whereas Cu^{2+} was adsorbed by PPy on the imine group, which further supports the hypothesis that Zn^{2+} and Pb^{2+} are more favored by TiO_2. From the XPS result, it can also be seen that the oxidation rate of PPy after adsorption decreased to around 20%, which can be attributed to the hydrolysis in the non-acid aqueous solution.

Taking the above into consideration, the mechanism for the synergistic adsorption on PPy/TiO_2 composite is proposed as follows: $TiO_2(O^-)$ together with SO_4^{2-} acted as the dopants for PPy and were involved in charge-transfer interactions within PPy in the PPy/TiO_2 system. After the composite was dosed with heavy metal ions from the solution at pH higher than 3, the exchange/dedoping process of dopants occurred. Some $TiO_2(O^-)$ ions were dedoped or exchanged by the counteranions (i.e., NO_3^-) in the solution with high concentration of NO_3^-.[50] After being dedoped, the negatively charged $TiO_2(O^-)$ needs to be electrically neutralized. In solutions at pH = 5, heavy metal ions would be preferentially attracted to $TiO_2(O^-)$ and the selective adsorption was mainly achieved at TiO_2 site, resulting in the interesting phenomenon that the selectivity of the composite is determined by TiO_2 instead of PPy. Therefore, PPy/TiO_2 composite displayed better affinity to Zn^{2+} and Pb^{2+} than Cu^{2+}, just as TiO_2 did. In other words, the novel selectivity is achieved through the synergistic adsorption between PPy and TiO_2. For the adsorption mechanism, according to our previous work,[15,16,29] hydroxyls become negatively charged after dedoping from PPy and electrostatically attracted heavy metal ions with positive charge. The electrostatic attraction was an important mechanism for the adsorption. In addition, the chelation of pyrrolylium nitrogen with lone pair electron to the heavy metal ions with unoccupied orbital could be another important mechanism for the adsorption after dedoping. Therefore, the adsorption mechanism could be expressed as follows

$$2\text{composite-O}^-(\text{hydroxyl}) + M^{2+}(\text{heavy metal ion}) \rightarrow 2\text{composite-O}^- \cdots M^{2+}\ (\text{electrostatic attraction}) \quad (6)$$

$$\text{composite-}N\text{: (pyrrolylium nitrogen)} + M^{2+}(\text{heavy metal ion}) \rightarrow \text{composite-}N\text{:} \rightarrow M^{2+}\ (\text{chelation}) \quad (7)$$

It should be noted that even though PPy had adsorption capacity to heavy metals through chelation, the loading of PPy was lower compared to TiO_2 from the TGA result. It can be concluded that the selective adsorption property of this PPy/TiO_2 composite was still determined by TiO_2.

We conducted the experiments by adjusting the pH of the solution (Figure S9) to confirm this synergistic mechanism. The adsorption capacities for Pb^{2+}, Zn^{2+}, and Cu^{2+} increased with the increased pH. It can be explained by that the dedoping of dopant and dopant exchange would be greatly improved at low concentration of H^+, resulting in the increased availability of $TiO_2(O^-)$ adsorption site and enhanced adsorption capacity for heavy metal ions.[26] In addition, the amount of imine group could be also increased at high pH, which may also increase the adsorption capacity.[29] All these results support the synergistic mechanism we proposed.

CONCLUSIONS

Herein, the mechanism on the synergistic adsorption between polymer and metal oxide in a polymer/metal oxide composite was proposed for the first time, as well as the self-doping nature of metal oxide on polymer. An interesting charge-transfer structure is formed between the coated PPy in its oxidized p-type doping state and TiO_2 in n-type state. This interaction results in the interesting selective adsorption property that Zn^{2+} can be selectively adsorbed with 77.81 mg/g adsorption capacity, whereas the adsorption for Cu^{2+} is totally suppressed in a multiple-heavy-metal-ion solution. The results from the FT-IR, XPS, and TGA confirm that the exchange/dedoping of $TiO_2(O^-)$ occurred during the adsorption process. The selectivity of the composite is determined by the component TiO_2. This proposed mechanism satisfactorily explains the interesting properties of the synergistic effect and the selective adsorption in PPy/TiO_2 system. This mechanism may also be applicable to other polymer/metal oxide composites where polymer can conduct doping−dedoping process, such as polythiophene and polyaniline. This work may also provide a guideline to get insight into the mechanism on the selective adsorption in other adsorbents. The low cost and easy recycling make the adsorption method very attractive for wastewater treatment. It should be also mentioned that Pb^{2+} and Zn^{2+} cannot be separated by PPy/TiO_2. The mechanism of special adsorption affinity of TiO_2 to Zn^{2+} and poor affinity to Cu^{2+} remains unknown. It may be related to the compatibility between the lattice structures of metal oxides and heavy metal ion hydroxide. Further investigation will be conducted in our future work in this case.

ASSOCIATED CONTENT

Supporting Information

The Supporting Information is available free of charge on the ACS Publications website at DOI: 10.1021/acs.langmuir.8b01987.

FT-IR spectra of PPy, TiO_2, and PPy/TiO_2 composite before and after Pb^{2+}, Zn^{2+}, and Cu^{2+} adsorption; TGA analysis of PPy, TiO_2, and PPy/TiO_2 composite before and after adsorption of Pb^{2+}, Zn^{2+}, and Cu^{2+}; EDS spectrum of the PPy/TiO_2 composite; XRD spectra of PPy, TiO_2, and PPy/TiO_2 composite; SEM (a) and TEM images before (b) and after (c) adsorption of mixture of Pb^{2+}, Zn^{2+}, and Cu^{2+}; single- and multicomponent adsorption isotherms for the adsorption of heavy metals onto the PPy/TiO_2 composite, PPy, and TiO_2, fitting with Langmuir model, Freundlich model, linear form of Dubinin−Radushkevich model and Temkin model; adsorption capacities of the PPy/TiO_2 composite for Pb^{2+}, Zn^{2+}, and Cu^{2+} in different initial pH; assignments of the FT-IR absorptions for PPy, TiO_2, and PPy/TiO_2 composite before and after adsorption of Pb^{2+}, Zn^{2+}, and Cu^{2+}; EDS element analysis of the PPy/TiO_2 composite; textural properties of PPy, TiO_2, and PPy/TiO_2 composite before and after adsorption; single- and multicomponent adsorption

DOI: 10.1021/acs.langmuir.8b01987
Langmuir 2018, 34, 10187−10196

isotherms parameters describing the adsorption of heavy metals (Pb^{2+}, Zn^{2+}, and Cu^{2+}) onto the PPy/TiO_2 composite, based on Dubinin−Radushkevich and Temkin models; adsorption performance of various sorbents for Pb^{2+}, Zn^{2+}, or Cu^{2+}; interconversions between the various redox states in PPy; calculation for the amount of SO_4^{2-} in the PPy chain; kinetic investigation; regeneration; field sample analysis (PDF)

AUTHOR INFORMATION

Corresponding Authors

*E-mail: fjtes@xjtu.edu.cn (J.F.).
*E-mail: yanwei@mail.xjtu.edu.cn (W.Y.).

ORCID

Jie Chen: 0000-0003-0724-6911
Caiyun Wang: 0000-0001-9539-2155
Jiangtao Feng: 0000-0002-8394-1724

Notes

The authors declare no competing financial interest.

ACKNOWLEDGMENTS

The authors gratefully acknowledge Esther Townsend for her kind help with the language and her helpful suggestions to improve the quality of our article. The authors gratefully acknowledge the Shaanxi Key research and development projects, China (Grant No. 2017SF-386) and the financial supports from the National Natural Science Foundation of China (Grant No. 21307098).

REFERENCES

(1) Isaac, R. A.; Gil, L.; Cooperman, A. N.; Hulme, K.; Eddy, B.; Ruiz, M.; Jacobson, K.; Larson, C.; Pancorbo, O. C. Corrosion in Drinking Water Distribution Systems: A Major Contributor of Copper and Lead to Wastewaters and Effluents. *Environ. Sci. Technol.* **1997**, *31*, 3198−3203.

(2) Voegelin, A.; Vulava, V. M.; Kretzschmar, R. Reaction-Based Model Describing Competitive Sorption and Transport of Cd, Zn, and Ni in an Acidic Soil. *Environ. Sci. Technol.* **2001**, *35*, 1651−1657.

(3) Celis, R.; HermosÍn, M. C.; Cornejo, J. Heavy Metal Adsorption by Functionalized Clays. *Environ. Sci. Technol.* **2000**, *34*, 4593−4599.

(4) Xu, Y.; Axe, L.; Yee, N.; Dyer, J. A. Bidentate Complexation Modeling of Heavy Metal Adsorption and Competition on Goethite. *Environ. Sci. Technol.* **2006**, *40*, 2213−2218.

(5) Liu, X.; Liu, M.; Zhang, L. Co-adsorption and sequential adsorption of the co-existence four heavy metal ions and three fluoroquinolones on the functionalized ferromagnetic 3D $NiFe_2O_4$ porous hollow microsphere. *J. Colloid Interface Sci.* **2018**, *511*, 135−144.

(6) Zare-Dorabei, R.; Ferdowsi, S. M.; Barzin, A.; Tadjarodi, A. Highly efficient simultaneous ultrasonic-assisted adsorption of Pb(II), Cd(II), Ni(II) and Cu (II) ions from aqueous solutions by graphene oxide modified with 2,2′-dipyridylamine: Central composite design optimization. *Ultrason. Sonochem.* **2016**, *32*, 265−276.

(7) Kang, E. T.; Neoh, K. G.; Tan, K. L. Polyaniline: A polymer with many interesting intrinsic redox states. *Prog. Polym. Sci.* **1998**, *23*, 277−324.

(8) Huang, J.; Zheng, Y.; Luo, L.; Feng, Y.; Zhang, C.; Wang, X.; Liu, X. Facile preparation of highly hydrophilic, recyclable high-performance polyimide adsorbents for the removal of heavy metal ions. *J. Hazard. Mater.* **2016**, *306*, 210−219.

(9) Li, Z.-J.; Huang, Z.-W.; Guo, W.-L.; Wang, L.; Zheng, L.-R.; Chai, Z.-F.; Shi, W.-Q. Enhanced Photocatalytic Removal of Uranium(VI) from Aqueous Solution by Magnetic TiO_2/Fe_3O_4 and Its Graphene Composite. *Environ. Sci. Technol.* **2017**, *51*, 5666−5674.

(10) Li, M.; Noriega-Trevino, M. E.; Nino-Martinez, N.; Marambio-Jones, C.; Wang, J.; Damoiseaux, R.; Ruiz, F.; Hoek, E. M. V. Synergistic Bactericidal Activity of Ag-TiO_2 Nanoparticles in Both Light and Dark Conditions. *Environ. Sci. Technol.* **2011**, *45*, 8989−8995.

(11) Fukahori, S.; Ichiura, H.; Kitaoka, T.; Tanaka, H. Photocatalytic Decomposition of Bisphenol A in Water Using Composite TiO_2-Zeolite Sheets Prepared by a Papermaking Technique. *Environ. Sci. Technol.* **2003**, *37*, 1048−1051.

(12) Hu, R.; Shao, D.; Wang, X. Graphene oxide/polypyrrole composites for highly selective enrichment of U(vi) from aqueous solutions. *Polym. Chem.* **2014**, *5*, 6207−6215.

(13) Khan, A. A.; Alam, M. M. Preparation, characterization and analytical applications of a new and novel electrically conducting fibrous type polymeric−inorganic composite material: polypyrrole Th(IV) phosphate used as a cation-exchanger and Pb(II) ion-selective membrane electrode. *Mater. Res. Bull.* **2005**, *40*, 289−305.

(14) Mahmud, H. N. M. E.; Huq, A. K. O.; Binti Yahya, R. The removal of heavy metal ions from wastewater/aqueous solution using polypyrrole-based adsorbents: a review. *RSC Adv.* **2016**, *6*, 14778−14791.

(15) Chen, J.; Feng, J.; Yan, W. Influence of metal oxides on the adsorption characteristics of PPy/metal oxides for Methylene Blue. *J. Colloid Interface Sci.* **2016**, *475*, 26−35.

(16) Chen, J.; Shu, C.; Wang, N.; Feng, J.; Ma, H.; Yan, W. Adsorbent synthesis of polypyrrole/TiO_2 for effective fluoride removal from aqueous solution for drinking water purification: Adsorbent characterization and adsorption mechanism. *J. Colloid Interface Sci.* **2017**, *495*, 44−52.

(17) Bonifas, A. P.; McCreery, R. L. Solid State Spectroelectrochemistry of Redox Reactions in Polypyrrole/Oxide Molecular Heterojunctions. *Anal. Chem.* **2012**, *84*, 2459−2465.

(18) Tan, K. L.; Tan, B. T. G.; Kang, E. T.; Neoh, K. G. Chemical nature of the nitrogens in polypyrrole and nitrogen-substituted polypyrrole: a comparative study by X-ray photoelectron spectroscopy. *J. Mater. Sci.* **1992**, *27*, 4056−4060.

(19) Bradl, H. B. Adsorption of heavy metal ions on soils and soils constituents. *J. Colloid Interface Sci.* **2004**, *277*, 1−18.

(20) Lim, C. W.; Song, K.; Kim, S. H. Synthesis of PPy/silica nanocomposites with cratered surfaces and their application in heavy metal extraction. *J. Ind. Eng. Chem.* **2012**, *18*, 24−28.

(21) Mahmud, H.; Hosseini, S.; Yahya, R. B. Removal of Nickel Ions from Aqueous Solution by Polypyrrole Conducting Polymer. *Key Eng. Mater.* **2014**, *594−595*, 793−797.

(22) Hosseini, S.; Ekramul Mahmud, N. H. M.; Binti Yahya, R.; Ibrahim, F.; Djordjevic, I. Polypyrrole conducting polymer and its application in removal of copper ions from aqueous solution. *Mater. Lett.* **2015**, *149*, 77−80.

(23) Lin, Y.; Cui, X.; Bontha, J. Electrically Controlled Anion Exchange Based on Polypyrrole and Carbon Nanotubes Nanocomposite for Perchlorate Removal. *Environ. Sci. Technol.* **2006**, *40*, 4004−4009.

(24) Li, J.; Feng, J.; Yan, W. Excellent adsorption and desorption characteristics of polypyrrole/TiO_2 composite for Methylene Blue. *Appl. Surf. Sci.* **2013**, *279*, 400−408.

(25) Ullah, H. Inter-molecular interaction in Polypyrrole/TiO_2: A DFT study. *J. Alloys Compd.* **2017**, *692*, 140−148.

(26) Tan, K. L.; Tan, B. T. G.; Kang, E. T.; Neoh, K. G. The chemical nature of the nitrogens in polypyrrole and polyaniline—a comparative-study by X-ray photoelectron-spectroscopy. *J. Chem. Phys.* **1991**, *94*, 5382−5388.

(27) Xu, J.; Yao, P.; Li, X.; He, F. Synthesis and characterization of water-soluble and conducting sulfonated polyaniline/para-phenylenediamine-functionalized multi-walled carbon nanotubes nanocomposite. *Mater. Sci. Eng., B* **2008**, *151*, 210−219.

(28) Yu, J. C.; Yu, J. G.; Ho, W. K.; Jiang, Z. T.; Zhang, L. Z. Effects of F^- doping on the photocatalytic activity and microstructures of nanocrystalline TiO_2 powders. *Chem. Mater.* **2002**, *14*, 3808−3816.

DOI: 10.1021/acs.langmuir.8b01987
Langmuir 2018, 34, 10187−10196

(29) Chen, J.; Wang, N.; Ma, H.; Zhu, J.; Feng, J.; Yan, W. Facile Modification of a Polythiophene/TiO2 Composite Using Surfactants in an Aqueous Medium for an Enhanced Pb(II) Adsorption and Mechanism Investigation. *J. Chem. Eng. Data* **2017**, *62*, 2208−2221.
(30) Kruk, M.; Jaroniec, M. Gas adsorption characterization of ordered organic-inorganic nanocomposite materials. *Chem. Mater.* **2001**, *13*, 3169−3183.
(31) An, H. K.; Park, B. Y.; Kim, D. S. Crab shell for the removal of heavy metals from aqueous solution. *Water Res.* **2001**, *35*, 3551−3556.
(32) Langmuir, I. The adsorption of gases on plane surfaces of glass, mica and platinum. *J. Am. Chem. Soc.* **1918**, *40*, 1361−1403.
(33) Freundlich, H. Concerning adsorption in solutions. *Z. Phys. Chem., Stoechiom. Verwandtschaftsl.* **1906**, *57*, 385−470.
(34) Dubinin, M. M.; Radushkevich, L. V. Equation of the characteristic curve of activated charcoal. *Proc. Acad. Sci., Phys. Chem. USSR* **1947**, *55*, 331.
(35) Temkin, M.; Pyzhev, V. Kinetics of ammonia synthesis on promoted iron catalysts. *Acta Phys. Chim. USSR* **1940**, *12*, 327−356.
(36) Keramat, A.; Zare-Dorabei, R. Ultrasound-assisted dispersive magnetic solid phase extraction for preconcentration and determination of trace amount of Hg (II) ions from food samples and aqueous solution by magnetic graphene oxide (Fe_3O_4@GO/2-PTSC): Central composite design optimization. *Ultrason. Sonochem.* **2017**, *38*, 421−429.
(37) Karthik, R.; Meenakshi, S. Chemical modification of chitin with polypyrrole for the uptake of Pb(II) and Cd(II) ions. *Int. J. Biol. Macromol.* **2015**, *78*, 157−164.
(38) Omraei, M.; Esfandian, H.; Katal, R.; Ghorbani, M. Study of the removal of Zn(II) from aqueous solution using polypyrrole nanocomposite. *Desalination* **2011**, *271*, 248−256.
(39) Zare-Dorabei, R.; Darbandsari, M. S.; Moghimi, A.; Tehrani, M. S.; Nazerdeylami, S. Synthesis, characterization and application of cyclam-modified magnetic SBA-15 as a novel sorbent and its optimization by central composite design for adsorption and determination of trace amounts of lead ions. *RSC Adv.* **2016**, *6*, 108477−108487.
(40) Kheibar, D.; Rouholah, Z.-D. An easily organic−inorganic hybrid optical sensor based on dithizone impregnation on mesoporous SBA-15 for simultaneous detection and removal of Pb(II) ions from water samples: Response-surface methodology. *Appl. Organomet. Chem.* **2017**, *31*, No. e3842.
(41) Xu, Z.; Wang, K.; Liu, Q.; Guo, F.; Xiong, Z.; Li, Y.; Wang, Q. A bifunctional adsorbent of silica gel-immobilized Schiff base derivative for simultaneous and selective adsorption of Cu(II) and SO_4^{2-}. *Sep. Purif. Technol.* **2018**, *191*, 61−74.
(42) Ali, J.; Wang, H.; Ifthikar, J.; Khan, A.; Wang, T.; Zhan, K.; Shahzad, A.; Chen, Z.; Chen, Z. Efficient, stable and selective adsorption of heavy metals by thio-functionalized layered double hydroxide in diverse types of water. *Chem. Eng. J.* **2018**, *332*, 387−397.
(43) Chandra, V.; Kim, K. S. Highly selective adsorption of Hg^{2+} by a polypyrrole−reduced graphene oxide composite. *Chem. Commun.* **2011**, *47*, 3942−3944.
(44) Oyetade, O. A.; Skelton, A. A.; Nyamori, V. O.; Jonnalagadda, S. B.; Martincigh, B. S. Experimental and DFT studies on the selective adsorption of Pb^{2+} and Zn^{2+} from aqueous solution by nitrogen-functionalized multiwalled carbon nanotubes. *Sep. Purif. Technol.* **2017**, *188*, 174−187.
(45) Chen, J.; Feng, J.; Yan, W. Facile synthesis of a polythiophene/TiO_2 particle composite in aqueous medium and its adsorption performance for Pb(II). *RSC Adv.* **2015**, *5*, 86945−86953.
(46) Li, Y. *Conducting Polymers*; Springer International Publishing, 2015; pp 23−50.
(47) Kim, C.-S.; Shin, J.-W.; Cho, Y.-H.; Jang, H.-D.; Byun, H.-S.; Kim, T.-O. Synthesis and characterization of Cu/N-doped mesoporous TiO_2 visible light photocatalysts. *Appl. Catal., A* **2013**, *455*, 211−218.
(48) Yoshida, T.; Yamaguchi, T.; Iida, Y.; Nakayama, S. XPS Study of Pb(II) Adsorption on γ-Al_2O_3 Surface at High pH Conditions. *J. Nucl. Sci. Technol.* **2003**, *40*, 672−678.
(49) Iaiche, S.; Djelloul, A. ZnO/$ZnAl_2O_4$ Nanocomposite Films Studied by X-Ray Diffraction, FTIR, and X-Ray Photoelectron Spectroscopy. *J. Spectrosc.* **2015**, *2015*, 1−9.
(50) Li, Y. F.; Qian, R. Y. Effect of anion and solution pH on the electrochemical-behavior of polypyrrole in aqueous-solution. *Synth. Met.* **1989**, *28*, 127−132.

DOI: 10.1021/acs.langmuir.8b01987
Langmuir 2018, 34, 10187−10196